Regenerative Therapy 19 (2022) 24–34

Contents lists available at ScienceDirect

Regenerative Therapy

journal homepage: http://www.elsevier.com/locate/reth

Original Article

Addition of Chk1 inhibitor and BMP4 cooperatively promotes retinal tissue formation in self-organizing human pluripotent stem cell differentiation culture

Suguru Yamasaki [a, b], Atsushi Kuwahara [b], Akiyoshi Kishino [b], Toru Kimura [b], Masayo Takahashi [a], Michiko Mandai [a, c, *]

[a] Laboratory for Retinal Regeneration, RIKEN Center for Biosystems Dynamics Research, Kobe, Hyogo, 650-0047, Japan
[b] Regenerative & Cellular Medicine Kobe Center, Sumitomo Dainippon Pharma Co., Ltd., Kobe, Hyogo, 650-0047, Japan
[c] RIKEN Program for Drug Discovery and Medical Technology Platforms (DMP), RIKEN Cluster for Science, Technology and Innovation Hub, Saitama, 351-0198, Japan

ARTICLE INFO

Article history:
Received 24 September 2021
Received in revised form
9 December 2021
Accepted 16 December 2021

Keywords:
Chk1 inhibitor
Pluripotent stem cell
Retina
Photoreceptor
Self-organization
Organoid
iPSC

ABSTRACT

Background: The BMP signaling pathway plays a key role in growth, differentiation and patterning during neural development. Recent work on the generation of a self-organization of three-dimensional retinal organoid (3D-retina) from human pluripotent stem cells (hPSCs) revealed that addition of recombinant human BMP4 (rhBMP4) promotes retinal differentiation in the early neural differentiation stage. For clinical application, efficient differentiation from hPSCs to retinal cells with minimal numbers of off-target non-retinal cells is desirable. We therefore aimed to further improve an efficient retinal differentiation method for future up-scaling of cell production.

Methods: hPSCs were differentiated into 3D-retina using a modified SFEBq method. The effect of rhBMP4 with or without Checkpoint kinase 1 (Chk1) inhibitor (PD407824), a modulator of BMP signaling pathway, at day 3 was compared by characterizing the differentiating 3D-retina by the use of the hPSCs and immunohistochemical analysis.

Results: The Chk1 inhibitor treatment promoted retinal differentiation from hPSCs, in combination with low-concentration rhBMP4. Addition of a Chk1 inhibitor generated a unique type of organoid with neural retina (NR) encapsulated in retinal pigment epithelium (RPE), possibly by promoting phosphorylation of SMAD1/5/9 in the cells inside the early aggregates. We confirmed that the Chk1-inhibitor-treated hPSC-3D-retina differentiated into rod and cone photoreceptor precursors and other types of retinal neurons, in long-term culture.

Conclusions: In this study, we found that combined use of rhBMP4 and a Chk1 inhibitor cooperatively promoted retinal differentiation from hPSCs. Our new retinal differentiation method is a promising option for the stable supply and up-scaling of production of 3D-retina for future cell therapy.

1. Introduction

Retinitis pigmentosa (RP) is a group of inherited, progressive diseases with photoreceptor degeneration that leads to loss of vision. Retinal transplantation is a possible therapeutic option for retinal degeneration with a severe loss of photoreceptors, and has been studied using laboratory animals [1–3]. Several clinical researches using fetal retina were performed during 1990s–2000s [4–6]. These studies provided clinical evidence of the safety of retinal transplantation, with possible potential for therapeutic

Abbreviations: BMP, Bone morphogenetic protein; Chk1i, Checkpoint kinase 1 inhibitor; PD, PD407824; RP, Retinitis pigmentosa; PSCs, Pluripotent stem cells; 3D-retina, three-dimensional retinal organoid.

* Corresponding author. Laboratory for Retinal Regeneration, RIKEN CBDR (Center for Biosystems Dynamics Research), 2-2-3 Minatojima-Minamimachi, Chuo-ku, Kobe, Hyogo 650-0047, Japan.
E-mail address: michiko.mandai@riken.jp (M. Mandai).

Peer review under responsibility of the Japanese Society for Regenerative Medicine.

https://doi.org/10.1016/j.reth.2021.12.003

benefits, but stable preparation of donor retinal tissue was still a major limitation in order to further assess treatment efficacy.

Human embryonic stem cells (hESCs) and induced pluripotent stem cells (hiPSCs) have great potential as an unlimited cell source of graft preparation. Eiraku et al. and Nakano et al. reported generation of a self-organizing 3D-retina derived from mouse and human ESCs, respectively, a major breakthrough in the clinical application of retinal transplantation [7,8]. Later, we reported that timed exogenous recombinant human BMP4 (rhBMP4) treatment in the early neural differentiation stage promoted highly selective retinal differentiation [9]. Other groups also reported the use of rhBMP4 for retinal differentiation, suggesting that BMP signaling pathway plays a key role in inducing retinal cells from human pluripotent stem cells (hPSCs) [10–12]. Recently, we optimized our method for retinal differentiation from feeder-free hPSCs, by preconditioning initial hPSC-state by modulating the levels of TGF-β superfamily signaling pathways and the sonic hedgehog signaling pathway [13]. Using these methods, the 3D-retina self-formed continuous retinal epithelium that differentiate into the neural retina (NR) and retinal pigment epithelium (RPE).

Several groups including ours have demonstrated that hPSC-derived retinal tissue sheet ('retinal sheet', hereafter) transplantation results in graft integration into the host retina with functional recovery, using end-stage retinal degeneration models in mice, rats and monkeys [14–19]. We recently demonstrated that hPSC-derived 3D-retina have low immunogenicity and immunosuppressive properties, a finding that is also advantageous for transplantation therapies [20]. These reports suggest the possible utility of hPSC-derived 3D-retinas in clinical usage intending to reconstitute retinal circuits.

For clinical application, an efficient and robust retinal differentiation method is important to prepare high-quality grafts. In general, some small molecules are more stable in solution than recombinant growth factors or trophic factors and their effect is highly reproducible. In addition, the regular use of rhBMP4 is expensive. We thus aimed to develop an improved retinal differentiation protocol for the efficient production of a 3D-retina, with reduced use of rhBMP4, to accommodate scaled-up cell production in the future. We focused to regulate Checkpoint kinase 1 (Chk1) during retinal differentiation. Chk1 was first identified as a serine/threonine cell cycle regulatory kinase that responds to DNA damage [21]. Chk1 inhibitor (Chk1i) have been well studied in cancer treatment that uses monotherapy or combination therapies [22]. Recently, Feng et al. identified a new role of Chk1i where it cooperated with rhBMP4 in promoting differentiation of mesoderm or cytotrophoblast stem cells from hESCs [23]. This report suggested that Chk1i PD407824 (PD) increased the sensitivity of cells to sub-threshold concentration of rhBMP4 during hESC differentiation. Therefore, Chk1i may have great potential to modulate the fate of various stem/progenitor cells in combination with the BMP signaling pathway. Our new method that uses timed treatment with the PD caused hPSCs to differentiate efficiently into a 3D-retina at a lower concentration (0.15 nM) of rhBMP4, compared to our previous protocol. Interestingly, 1.5 nM rhBMP4 and Chk1i treatment generated NR-RPE organoids with NR tissue encapsulated within the RPE, possibly by enhancing BMP signaling in the inner cells of the early aggregates.

2. Materials and methods

2.1. Maintenance of human ESCs and iPSCs

hESCs (KhES-1) that express *Venus* under the control of the *Rx* promoter [8] were used according to the hESC research guidelines of the Japanese government, and cultured at RIKEN. hiPSCs (1231A3) were established by Kyoto University and derived from ePBMC(R) purchased from Cellular Technology Limited (http://www.immunospot.com/), and provided by Kyoto University [24]. hESCs and hiPSCs were maintained in StemFit medium (Ajinomoto, Japan) in six-well tissue culture plates (AGC Techno Glass, Japan) coated with LM511-E8 matrix (iMatrix511, Matrixome, Japan) as previously described [24]. The medium was changed (1.5–2 mL/well) every 1–2 days until approximately 70–80% confluence was reached. After washing with PBS, cells were enzymatically passaged using TrypLE Select Enzyme (Thermo Fisher Scientific) and 1.0–1.2 × 10^4 cells were plated in each well of six-well, LM511-E8 coated plates containing StemFit medium with 10 μM Y-27632 (Wako Pure Chemical Industries, Japan). From the following day, the medium was replaced to StemFit medium without Y-27632. All cells were cultured at 37 °C with 5% CO_2.

2.2. Chemicals used in combination with rhBMP4

SB-4 (#6881) and PD407824 (#2694) were purchased from R&D Systems. SJ0002919 was purchased from Sigma–Aldrich (#SML2087). These compounds were dissolved in DMSO (Wako) and stored at −30 °C.

2.3. Retinal differentiation from human ESCs and iPSCs

hESCs and hiPSCs were differentiated into a 3D-retina using a modified "serum-free floating culture of embryoid body-like aggregates with quick reaggregation (SFEBq)" method combined with preconditioning as we previously reported [9,13,20]. For one day prior to differentiation, hESCs and hiPSCs were treated with 5 μM SB431542 (TGF-β receptor inhibitor, Wako Pure Chemical Industries) and 300 nM SAG (smoothened agonist, Enzo Biochem) in StemFit medium as described previously [13]. The following day, hESCs and hiPSCs were placed in differentiation medium (gfCDM) supplemented with Y-27632 and SAG in low-cell-adhesion, 96-well V-bottomed plates (Sumilon Prime Surface plate: Sumitomo Bakelite; 1.2 × 10^4 cells/well). The differentiation medium (gfCDM) comprised Ham's F12 (Thermo)/Iscove's modified Dulbecco's medium (Thermo) 1:1, 10% KSR (Thermo), 1% Chemically defined lipid concentrate (Thermo) and 450 μM Monothioglycerol (Sigma). At day 3, rhBMP4 and 1 μM PD (Chk1i) were added to the differentiation medium. The rhBMP4 and 1 μM PD concentration were reduced in a step-wise manner by replacing half the medium. The differentiation medium was changed every 3–4 days until the next induction-reversal culture step. Induction-reversal culture and long-term maturation culture were performed as described [9,13,20] (WO2019017492A1, WO2019054514A1).

2.4. Immunohistochemistry and imaging

Immunohistochemistry protocols were performed as previously described [20]. The differentiated 3D-retinas were fixed with 4% paraformaldehyde (Wako Pure Chemical Industries) at 4 °C for 15 min and washed with PBS, and then equilibrated in 20% sucrose/PBS solution at 4 °C overnight. 3D-retina were embedded in OCT compound (Sakura Finetek Japan), and sectioned at 12 μm thickness using a cryostat (Leica Camera). Sections were treated with or without heat-induced epitope retrieval using citrate buffer. Primary antibodies used in this study are summarized in Table 1. All images were obtained using TSC SP-8 (Leica Camera) or LSM880 (Carl Zeiss) laser scanning confocal microscopes. Images were processed using Imaris and Zen Blue (Carl Zeiss) imaging software.

2.5. Statistical analysis

Statistical analyses were performed with Excel software. Data represent mean ± s.e.m.

Table 1
Antibodies.

Antigen	Host	Source	Cat No.	RRID	Dilution
Brn3	Goat	Santa Cruz Biotechnology	sc-6026	AB_673441	1:200
Calbindin	Rabbit	Abcam	ab108404	AB_10861236	1:500
Chx10	Mouse	Santa Cruz Biotechnology	sc-365519	AB_10842442	1:500
Chx10	Sheep	Exalpha Biologicals	X1180P	AB_2314191	1:500
Collagen-IV	Rabbit	Abcam	ab6311	AB_305414	1:500
Crx	Rabbit	Takara Bio Inc.	M231		1:500
EphrinB2	Goat	R&D Systems	AF496	AB_2095679	1:500
Laminin	Rabbit	Abcam	ab-11575	AB_298179	1:500
Mitf	Mouse	Exalpha Biologicals	X2398M		1:500
Nrl	Goat	R&D Systems	AF2945	AB_2155098	1:500
Ki67	Rabbit	R&D Systems	MAB7617		1:500
Pax6	Mouse	BD Pharmingen	561462	AB_10715442	1:500
Pmel17	Rabbit	Abcam	ab137062		1:500
pSMAD1/5/9	Rabbit	Cell Signaling Technology	13820S	AB_2493181	1:500
Recoverin	Rabbit	Proteintech	10073-1-AP	AB_2178005	1:500
Rx	Guniea pig	Takara Bio Inc.	M229		1:500
Rxrγ	Mouse	Santa Cruz Biotechnology	sc365252	AB_10850062	1:500
Sox2	Mouse	BD Pharmingen	561469	AB_10694256	1:500
TBX5	Rabbit	Novus Biologicals	NBP1-83237	AB_11018767	1:500
Zo-1	Mouse	Invitrogen	33–9100	AB_87181	1:500
Zo-1	Rabbit	Invitrogen	61–7300	AB_138452	1:500

3. Results

3.1. Chk1i PD407824 combined with rhBMP4 promoted Rx::Venus induction

We aimed to further improve an efficient retinal differentiation method for future up-scaling of cell production. We first investigated whether a small molecule can enhance retinal differentiation either alone or in combination with rhBMP4. We examined the effect of three candidate BMP signal activators at two concentrations; SB-4 [25], SJ000286237 [26] and PD407824 (PD) [23]. Using hESC line (KhES-1) with *Venus* cDNA knocked in the locus of the retinal progenitor marker Rx [27], we evaluated retinal differentiation by the induction of *Rx::*Venus expression, following a self-organizing retinal differentiation protocol SFEBq with some modifications that used preconditioning and BMP4 methods (Fig. 1A) [7–9,13]. On day 9, none of these small molecules induced *Rx::*Venus expression when applied alone (Fig. 1B). However, the addition of 1 μM PD combined with 0.15 nM rhBMP4 strongly induced *Rx::*Venus in the whole aggregate (Fig. 1C). We also found that treatment with 1.5 nM rhBMP4 and 1 μM PD on the aggregate on day 3 promoted self-formation of *Rx::*Venus positive inner aggregates. The timing of PD treatment was found to be important; for example, hESC-derived aggregates on day 12 collapsed when 1 μM PD was applied from the beginning of the differentiation culture (Figure S1A). These observations suggested that simultaneous treatment with rhBMP4 and PD effectively promoted retinal differentiation.

3.2. Chk1i PD407824 combined with low-concentration rhBMP4 treatment efficiently differentiates 3D-retina

Next, we evaluated whether the differentiation method with 0.15 nM rhBMP4 + 1 μM PD can induce 3D-retina, like our previous method with 1.5 nM rhBMP4. Most aggregates differentiated into a *Rx::*Venus positive hESC-derived 3D-retina on day 14 with both the 1.5 nM rhBMP4 and the 0.15 nM rhBMP4 + 1 μM PD differentiation methods (Fig. 2A). The 3D-retina often presented with lobular vesicle structures and with *Rx::*Venus-negative cell clumps attached by the 1.5 nM rhBMP4 method, while these *Rx::*Venus-negative cell clumps were rarely observed by the 0.15 nM rhBMP4 + 1 μM PD differentiation method (Fig. 2B). This result suggested that low-concentration rhBMP4 + PD treatment enhanced efficient retinal differentiation.

3.3. Generation of a NR-RPE organoid with NR tissue encapsulated within the RPE

At our screening of small molecules in combination with rhBMP4, on day 9 *Rx::*Venus positive inner aggregates were observed under treatment with 1.5 nM rhBMP4 and 1 μM PD (Fig. 1C). The differentiation step called 'induction-reversal' culture was performed from day 14 as a part of our regular protocol [9]. In this process, the GSK3β inhibitor CHIR99021 and the FGF receptor inhibitor SU5402 were applied for 3–4 days from days 14–18; with the induction of RPE-prone cells from retinal progenitor cells, followed by the reversal to NR epithelium. After induction-reversal culture, hESC-derived 3D-retina formed a capsule-like superficial layer of pigmented cells (Fig. 3A). Importantly, *Rx::*Venus positive NR self-formed in the pigmented cells capsule after the reversal culture process (Fig. 3B). On day 21, we then characterized the 3D-retinas using immunohistochemistry on frozen sections. Chx10 positive NR progenitor cells spontaneously formed NR epithelium within the Mitf positive RPE capsule (Fig. 3C). Notably, we frequently observed a tapering epithelial morphology at the boundary between NR and RPE, which resembled the morphology of the ocular ciliary margin (CM) in vivo (Fig. 3C and Figure S1) [9]. Furthermore, serial section staining with an apical marker Zo-1 and a basal marker collagen-IV revealed that these NR tissue encapsulated within the RPE (NR-RPE organoids, hereafter) exhibited a continuous epithelial structure with apico-basal polarity (Fig. 3D). In the NR-RPE organoids, the Zo-1 was localized on the apical side of *Rx::*Venus positive NR progenitor cells and the outer surface of RPE, while the Collagen-IV positive basement membrane was located on the inner capsule. Later, on day 60, Chx10 positive NR progenitor cells constituted the largest population and Crx positive photoreceptor precursors accumulated in the most apical layer, occasionally facing the pigmented RPE (Fig. 3E). These observations show that the new 1.5 nM rhBMP4 + 1 μM PD differentiation method can generate a unique NR-RPE organoids with NR tissue encapsulated in the RPE.

3.4. Chk1i PD407824 causes distributional changes of proliferating cells and may enhance BMP signaling inside the aggregate

Since Chk1 is known to be involved in cell cycling, we examined the effect of PD on cell proliferation in aggregates [21]. The PD treatment tended to result in hiPSC-derived aggregates with a

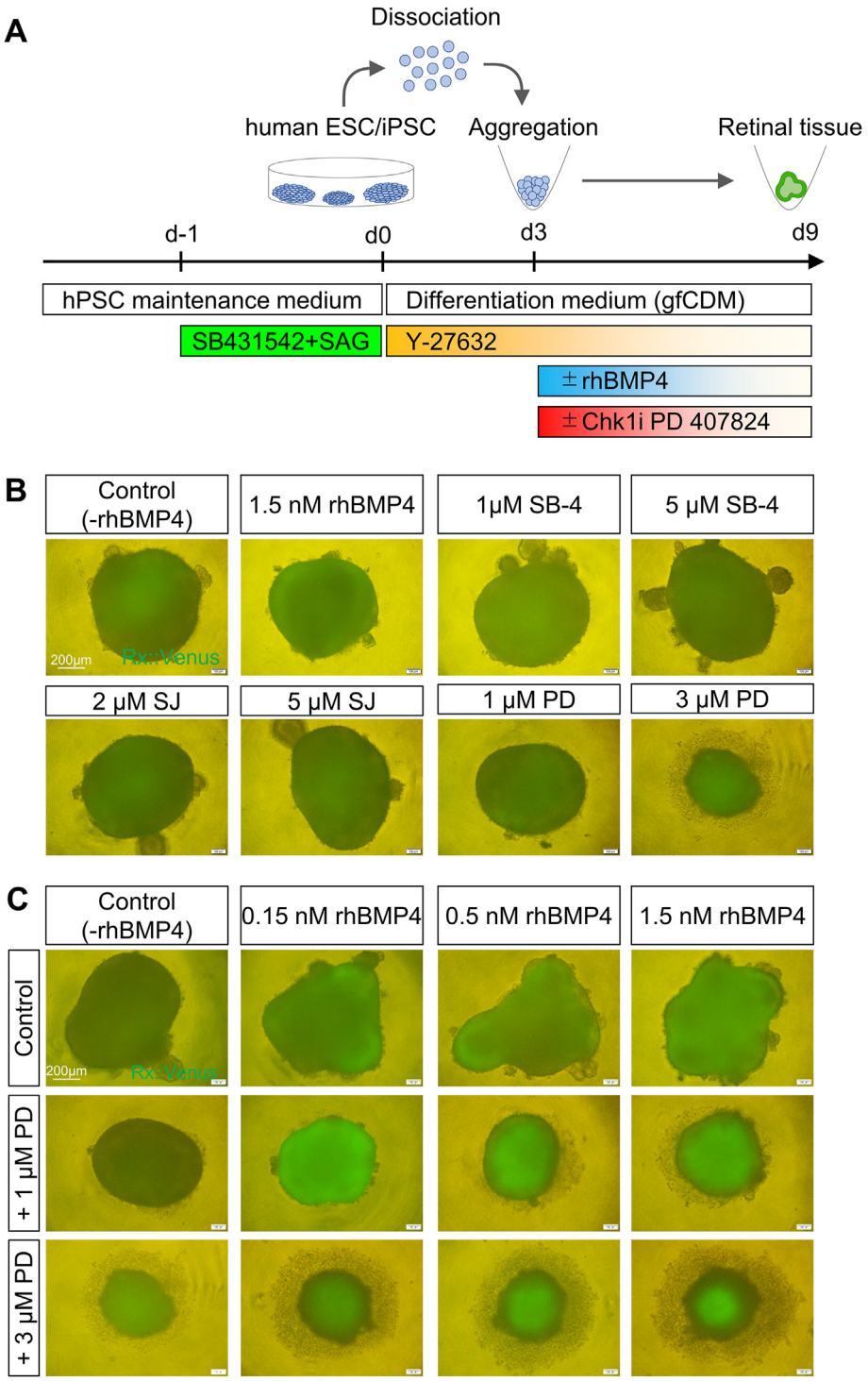

Fig. 1. Chk1i PD407824 combined with rhBMP4 treatment promotes retinal differentiation from hESCs. (A) Scheme of retinal differentiation. rhBMP4 and 1 μM PD (Chk1i) were added in the differentiation medium on day 3. The concentration of rhBMP4 and PD were diluted into half by half medium change on every 3–4 days. (B-C) Examination of three candidate small molecule BMP signal activators for induction of *Rx*::Venus expression using hESCs *Rx*::Venus reporter line. Bright-field view with expression of *Rx*::Venus of day 9 aggregates after small molecule treatment. (B) Treatment with small molecules alone. (C) PD treatment combined with rhBMP4. Scale bar, 200 μm (B, C), SJ: SJ000286237, PD: PD407824.

small spherical shape compared to non-PD-treated aggregates that formed a lobulated appearance on day 6 (Fig. 4A). The spherical shape was relatively maintained in 1.5 nM rhBMP4 + 1 μM PD-treated aggregates on day 17 before induction-reversal culture step (Fig. 4B). With immunohistochemical analysis, the number of proliferation marker Ki67 positive cells was decreased in PD-treated aggregates in the outer layer on day 6 (Fig. 4C). On day 17, Ki67 positive cells in outer neural epithelium were not much different between PD-treated and non-treated-aggregates but were observed inside the aggregate with 1.5 nM rhBMP4 and PD-treated aggregates (Fig. 4D). These results suggested the localization change in proliferating types of cells by PD in retinal differentiation culture.

To examine whether PD affects the effector molecules in BMP signaling pathway, we observed the localization of phosphorylated

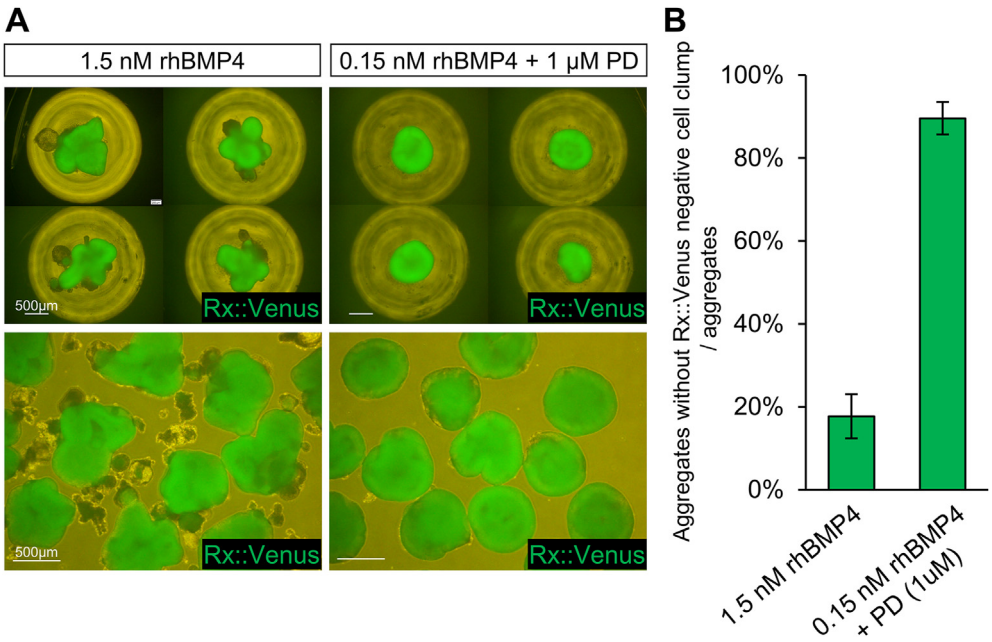

Fig. 2. Treatment with low-concentration rhBMP4 and Chk1i PD407824 efficiently causes retinal differentiation reducing an *Rx*::Venus-negative cell clumps. (A) Bright-field view with *Rx*::Venus fluorescence in hESC-derived 3D-retina on day 14. Images were obtained on an individual low cell binding 96-well V-bottomed plate (upper image) or a 90 mm Petri dish after the transfer for long-term culture (lower image). (B) Quantification analysis of 3D-retinas without an *Rx*::Venus-negative cell clump. Data represent mean ± s.e.m. (n = 3 with 32 3D-retinas). Bars represent the proportion of the 3D-retina without a non-retinal cell clump. Scale bars, 500 μm.

Smad1/5/9 (pSmad1/5/9) in aggregates of day 6 and day 17. Compared to control (-rhBMP4) aggregates, phosphorylation of SMAD1/5/9 was enhanced in rhBMP4-treated aggregates (Fig. 5A and B). Although pSmad1/5/9 positive cells were limited to the outer continuous epithelial layer in 1.5 nM rhBMP4-treated aggregates, pSmad1/5/9 positive cells were observed not only in the outer layer but also inside the aggregates in 1.5 nM rhBMP4 and PD-treated aggregate (Fig. 5A and B). Concomitantly, on day 17, NR progenitor marker Chx10 was also positive in both outer and inner cells in 1.5 nM rhBMP4 and PD-treated aggregates (Fig. 5B).

We also examined the expression of T-box 5 (Tbx5) and EphrinB2, which are downstream target of BMP signaling during the retinal development in vivo [28,29]. In 1.5 nM rhBMP4 treated aggregate, Tbx5 and EphrinB2 were expressed in outer NR layer (Fig. 5C and Figure S2), while Tbx5 and EphrinB2 were co-expressed in outer-layer cells as well as in the folded NR layers inside the aggregate after treatment with 1.5 nM rhBMP4 + PD. These implied the activation of the downstream effector molecules of BMP signaling both outside and inside the aggregate by PD, which may lead to NR tissue formation inside the aggregate. Moreover, aggregate formed apico-basal polarity, expressing Laminin on the basal side and Zo-1 on the apical side at early differentiation stage (Fig. 5D and E). Surprisingly, PD treated aggregates were packed with folded NR with Zo-1 positive apical vacuoles inside. These findings raise a possibility that the treatment of PD may lead to NR-RPE organoids formation by causing a distributional change in proliferating cells as well as by enhancement of BMP signaling inside the aggregate.

3.5. The Chk1i PD407824-treated hESC-3D-retina forms a multilayer and differentiates into rod and cone photoreceptor precursors in long-term culture in vitro

Finally, we evaluated the potential for PD-treated 3D-retina undergoing long-term *in vitro* culture to differentiate into each type of retinal cell, including rod and cone photoreceptor precursors. After induction-reversal culture, hESC-derived 3D-retina was further cultured for 42 days, as described previously [20]. During a long term culture, NR tissues expanded and often grew out of RPE capsule of the NR-RPE organoid that was initially formed in 1.5 nM rhBMP4 + PD (Figure S1B). On day 60, the 3D-retina treated with 0.15 nM rhBMP4 + PD had formed *Rx*::Venus positive NR epithelium similar to control 1.5 nM rhBMP4-treated 3D-retina (Fig. 6A-A′). In contrast, 3D-retina treated with 1.5 nM rhBMP4 + PD were reproducibly observed to contain pigmented RPE tissue (Fig. 6A-A′). These observations were also seen at day 136, on further long-term culture (Fig. 6B-B'). With immunohistochemical analysis, we found Pmel17 positive RPE tissue was observed in 3D-retina treated with 1.5 nM rhBMP4 + PD, on both days 60 and 136 (Fig. 6C and D). Sox2 positive/Ki67 positive/Chx10 positive NR progenitor cells formed on the inner neuroblastic layer and this NR progenitor cells population had significant decreased on day 136 (Fig. 6E–H). In contrast, photoreceptor precursor marker Crx positive and bona fide pan-photoreceptor marker recoverin positive photoreceptors had differentiated and accumulated in the apical-most outer layer on day 136 (Fig. 6I and J). Early cone marker Rxrγ positive cone photoreceptor precursors were observed from day 60, and later on day 136, with expression of the arrestin-3 cone photoreceptor marker (Fig. 6K-L and Figure S3A). Rod-specific transcription factor Nrl positive rod photoreceptor precursors were observed from day 136 (Fig. 6L). Nrl positive rod nuclei were located on the inner side of Rxrγ positive cone nuclei in the densely packed ONL-like structure. In addition, Brn3 positive retinal ganglion cells, calbindin positive horizontal cells, calretinin positive amacrine cells, and PKCα positive bipolar cells were observed on the basal side of PD-treated 3D-retina (Figure S3B-E). These immunohistochemical observations demonstrated that the rhBMP4 and PD-treated 3D-retina has the ability to produce retinal cells including rod and cone photoreceptor precursors, with multiple stratified layers.

4. Discussion

A method for efficient retinal differentiation is mandatory for future, scalable manufacturing for retinal cell therapy. In this study, by screening for candidate BMP signal activators, we found that

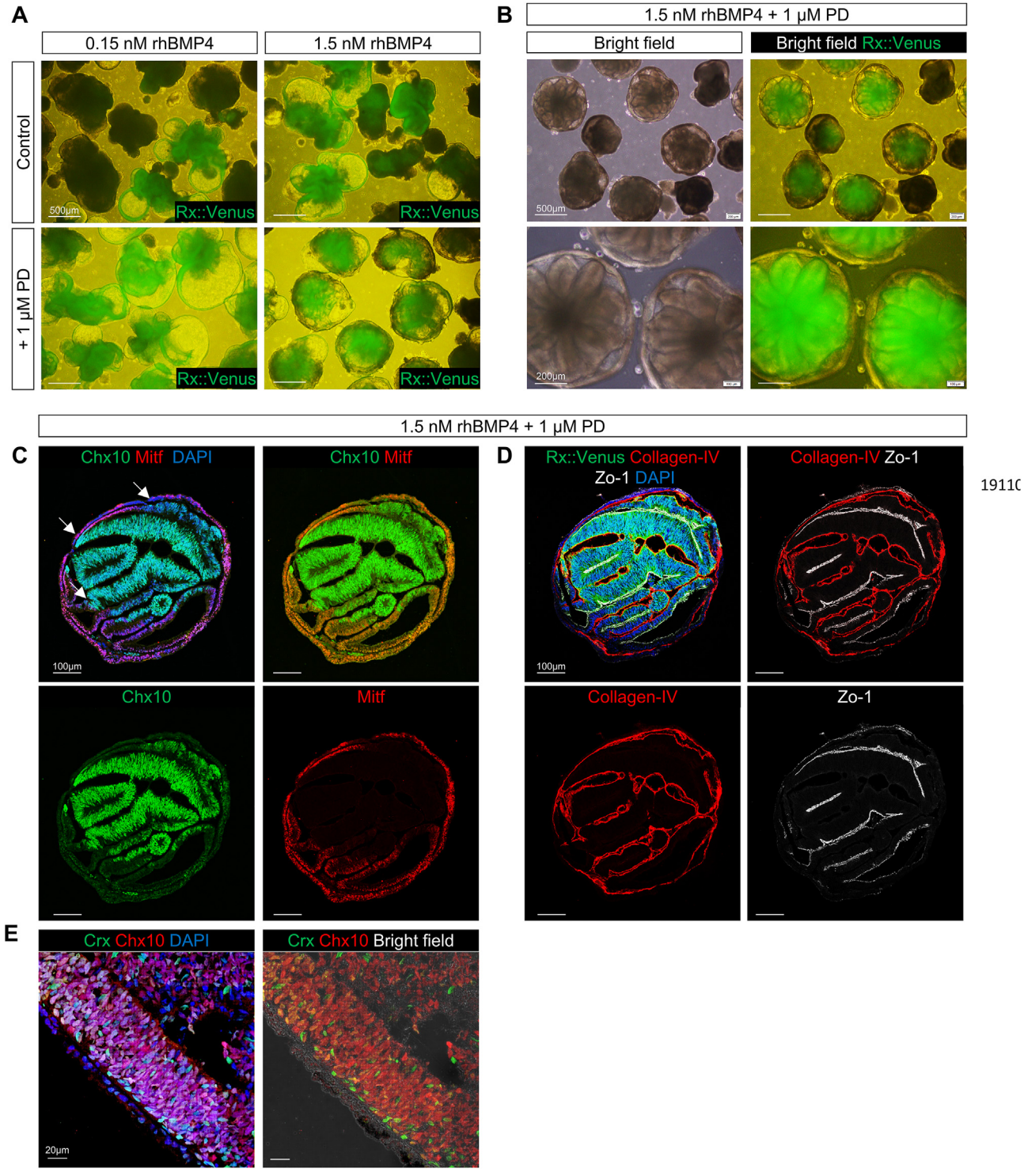

Fig. 3. Selective induction of NR-RPE organoids with NR tissue encapsulated in RPE under treatment with 1.5 nM rhBMP4 and Chk1i PD407824. (A) Bright-field with *Rx::*Venus fluorescence image of hESC-derived 3D-retinas on day 17. Note that low-concentration (0.15 nM) rhBMP4 and PD treatment in 3D-retina efficiently promoted formation of *Rx::*Venus-positive 3D-retinas compared to the 0.15 nM rhBMP4 treatment alone (control). (B) 1.5 nM rhBMP4 + PD-treated day 21 3D-retinas show self-organized, *Rx::*Venus-expressing NR tissue in these pigmented spheres. (C-D) Immunostaining of day 21 NR-RPE organoids for Chx10 (NR progenitor cells; green), Mitf (RPE; red), Zo-1 (Apical; white) and Collagen-IV (basement membrane; red) with DAPI nuclear staining (blue). (C) Chx10 positive NR progenitor cells were located in the Mitf positive RPE capsule. Arrows indicate the tapering structure of the NR-RPE junction. (D) Zo-1 and Collagen-IV immunostaining show the spontaneously developed apico-basal polarity in NR-RPE organoids. (E) Immunostaining of 1.5 nM rhBMP4 + PD-treated NR-RPE organoids for Crx (photoreceptor precursor cells; green) and Chx10 (NR progenitor cells; red) on day 60. Crx positive photoreceptor precursors located and accumulated in the most apical layer facing the RPE. Scale bars, 500 μm (A, B upper image), 200 μm (B, lower image), 100 μm (C-D), 20 μm (E).

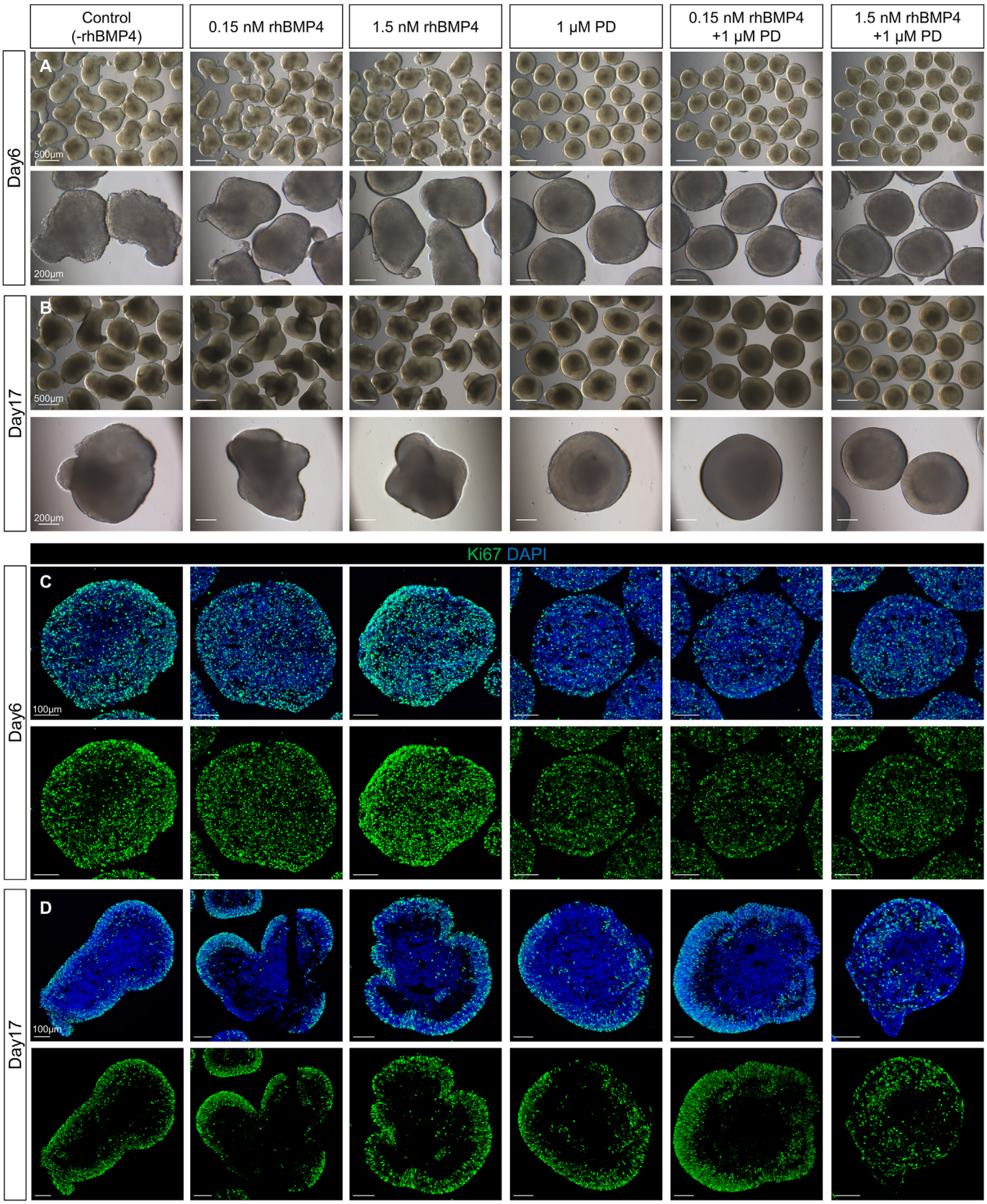

Fig. 4. An addition of Chk1i PD407824 directs the aggregates to form spherical morphology with a distributional change in proliferating cells. (A-B) Representative hiPSC-derived aggregate images of day 6 and day17 with the indicated rhBMP4 and PD concentrations. Aggregates of all six differentiation conditions formed epithelial structure. PD-treated aggregates (+PD, 0.15 nM BMP4 + PD, 1.5 nM BMP4 + PD) show a spherical morphology compared to the non-treated condition. (C-D) Immunostaining for Ki67 (green) to analyze the distribution of proliferating cells in the day 6 and day 17 aggregates. Blue, nuclear staining with DAPI. Scale bars, 500 μm (A. upper image), 200 μm (A, lower image), 100 μm (C-D).

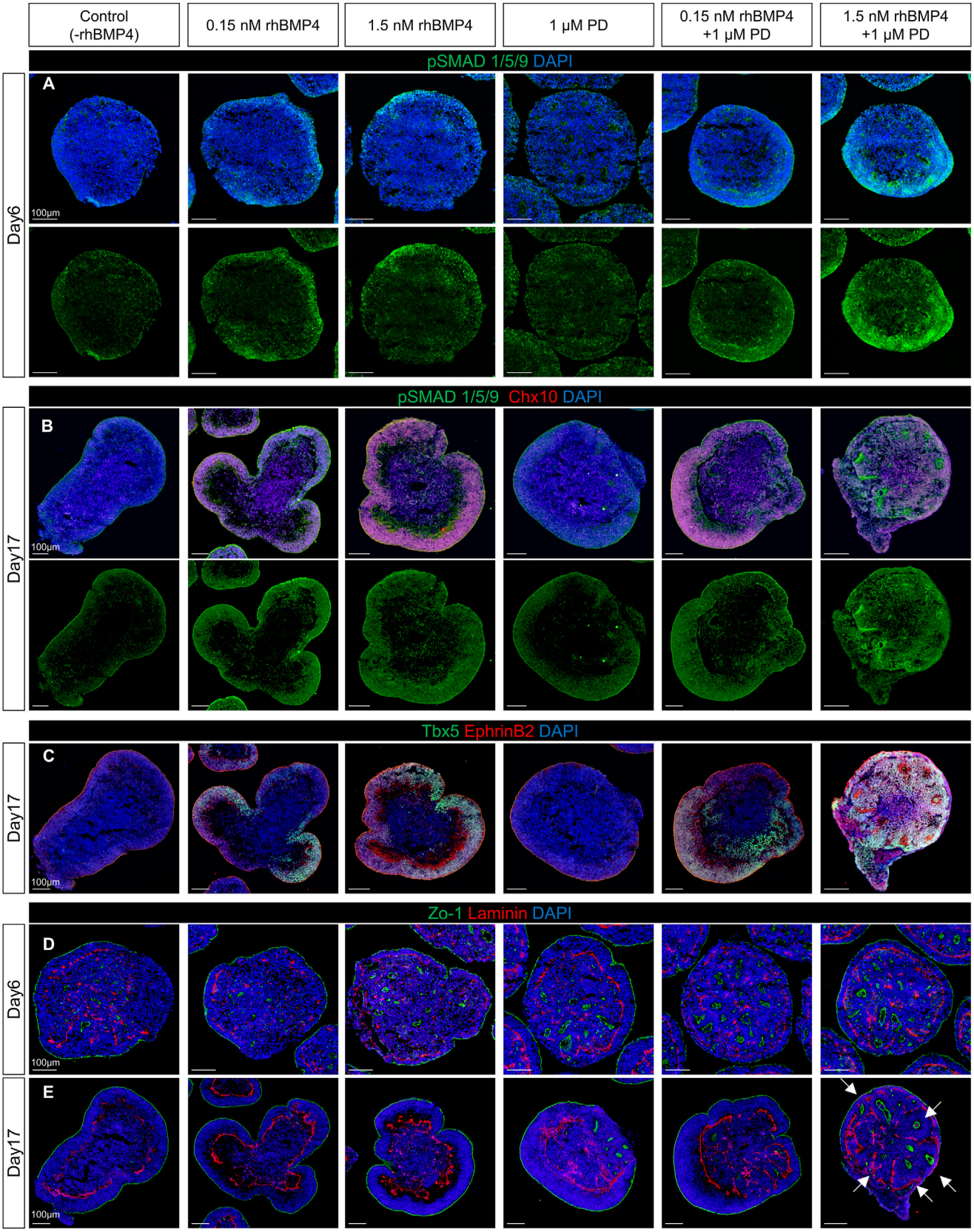

Fig. 5. Chk1i PD407824 and rhBMP4 promotes phosphorylation of SMAD1/5/9 toward inside the aggregates concomitantly with NR formation. (A-B) Representative confocal images of day 6 and day17 hiPSC-derived aggregate staining for pSmad1/5/9 (green) and NR progenitor markder Chx10 (red). Blue, nuclear staining with DAPI. (C) Immunostaining for Tbx5 (green) and EphrinB2 (red), the downstream of BMP signaling during retinal development in vivo. (D-E) Apical marker Zo-1 (green) and basement membrane marker Laminin (red) immunostaining show the apico-basal polarity in day 6 and day 17 aggregates. Arrows indicate self-organized NR tissues within aggregate. Scale bars, 100 μm (C).

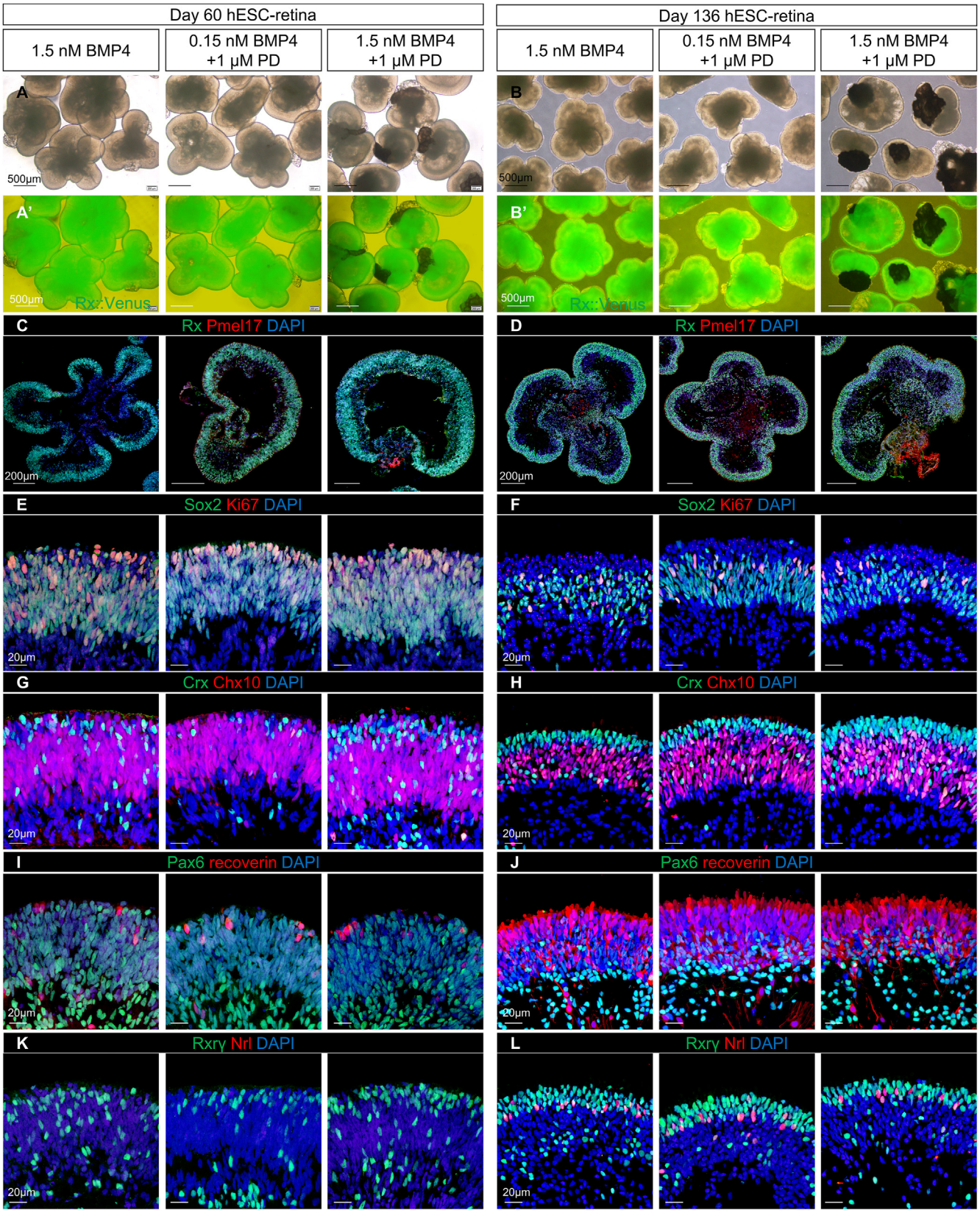

Fig. 6. Chk1i PD407824-treated 3D-retina has the ability to produce retinal cells, retinal ganglion cells, horizontal cells, and cone and rod photoreceptor precursors. (A, B) Bright-field view with *Rx::*Venus fluorescence in PD-treated or non-treated hESC-3D-retina on days 60 (A′) and 136 (B′). Note that a stratified, continuous NR epithelium was maintained in PD-treated 3D-retina during long-term maturation culture. (C-L) Immunostaining of the hESC-3D-retina with antibodies for (C, D) Rx (green) and Pmel17 (red), (E-F) Sox2 (green) and Ki67 (red) (G-H) Crx (green) and Chx10 (red) (I-J) Pax6 (green) and recoverin (red) (K, L) Rxrγ (green) and Nrl (red). Blue, nuclear staining with DAPI. (C, E, G, I, K) Day 60. (D, F, H, J, L) Day 136. Scale bars, 500 μm (A), 200 μm (B), 20 μm (E-L).

combined treatment of rhBMP4 and Chk1i PD407824 promoted retinal differentiation. Lower concentrations (0.15 nM) of rhBMP4 with PD treatment generated 3D-retina with expression of *Rx::*Venus, without the lobular vesicle structures and frequent *Rx::*Venus-negative cell clumps that were found in controls differentiated with the 10-fold higher concentration of rhBMP4 used in our previous method. We further demonstrated that combined treatment of 1.5 nM rhBMP4 and Chk1i promoted self-formation of NR-RPE organoids with NR tissue encapsulated in RPE. This study suggests that the combined rhBMP4 and Chk1i retinal differentiation method would be useful for scaling culture in clinical manufacturing by reducing the amount of rhBMP4 that is used.

In general, scalable production of grafts derived from stem cells, for use in transplantation therapy, requires stable supply of adequate amounts of high-quality cells with rigorous production processes adapted to Good Manufacturing Practice (GMP) standards. In addition, since cell-based products are generally expensive, the manufacturing steps are desired to provide a cost-effective platform in respect of medium, scaffold and recombinant proteins. It is well known that one of the expensive reagents used during the cell production step is recombinant proteins. Therefore, replacement of recombinant proteins with small molecules is ideal in any differentiation protocol. Small molecules that are potentially useful for modulating BMP signaling include BMP signal inhibitors such as LDN-193189, dorsomorphin and DMH1. Although some small molecules have been reported to be BMP signaling activators, Feng et al. reported most of the identified molecules have low activity and fail to induce mature osteoblasts in the absence of exogenous rhBMP addition. Our results also demonstrated that treatment with small molecules alone did not induce expression of *Rx::*Venus retinal progenitor cells. It may be difficult to activate BMP signaling strongly using a small molecule alone. Therefore, the use of a small molecule in combination with low-concentration rhBMP protein may be the most practical way to enhance BMP signaling pathway. Our study will help efficient production of retinal tissues or cells from hPSC for both research and clinical use.

BMP signaling is a key factor for the induction of differentiation of various cells such as trophoblasts and mesodermal cells [30,31], maintaining pluripotency and self-renewal [32]. In our SFEBq neural differentiation system, we applied rhBMP4 treatment to differentiate hPSC into the retinal fate efficiently. Chk1i may useful for rhBMP4 based differentiation methods, not just in previously reported mesoderm or cytotrophoblast lineage differentiation systems [23] but also for our retinal differentiation systems. In addition, complex organoids containing several tissues might possibly be generated depending on the concentration, timing, and duration of treatment with rhBMP4.

Much progress has been made in producing retinal differentiation methods over the decade. In contrast, little is known about how to regulate 3D patterns of morphology and shape in the retina. In our BMP4-treated retinal differentiation method, lobular vesicular structures were routinely observed. In contrast, PD-treated aggregates formed a spherical shape regardless of the presence or absence of rhBMP4. These observations suggested that Chk1 may play an important role for 3D-patterning of aggregates.

Previously, Feng et al. suggested a mechanism where Chk1i indirectly sensitized BMP signaling [23]. According to this report, Chk1 inhibition causes downregulation of p21, leading to activation of CHK8/9 and ultimately, enhanced SMAD2/3 degradation. Consequently, BMP ligands effectively activate targets downstream of BMP through SMAD1/5/9, associated with an increase in available SMAD4. In the present study, we did not devote much attention to the mechanism of BMP signaling, however, we were able to cause efficient differentiation of a 3D-retina, even with the use of low concentrations of rhBMP4 and PD. Although a similar BMP sensitizing mechanism was thus considered to be present with our retinal differentiation, Chk1i may still cause regulation of 3D aggregate patterning apart from BMP signaling.

Intriguingly, 1.5 nM rhBMP4 and Chki1i treatment generated NR-RPE organoids with NR tissue encapsulated in RPE. One possible mechanism for generation of such NR-RPE organoids may be due to the sensitization of BMP signaling pathway inside the aggregate by Chk1i, as was implied by the presence of the inner cells that were positive for phosphorylated Smad1/5/9 and Tbx5/EphrinB2. The reason why inner cells of the aggregate expressed phosphorylated Smad1/5/9 and Tbx5/EphrinB2 after treatment with the addition of PD still remains unclear. Considering the molecular weight (MW) and permeability of rhBMP4, a rhBMP4 decreasing concentration gradient would likely exist in the direction of the inner aggregate. In the absence of PD conditioning, the inner concentration of rhBMP4 might not reach the threshold for BMP signaling activation. However, it is possible that a mechanism exists that permits activation of BMP signaling in the inner cells, even with low concentrations of exogenous rhBMP4, due to the increased sensitivity of those inner cells to sub-threshold concentration of rhBMP4 by PD. Differences in the inner and outer microenvironment, such as rhBMP4 concentration gradients within the aggregate, may lead to changes in the fate of cells, with differentiation of early retinal progenitor cells into NR or RPE cells.

5. Conclusions

We found that the Chk1i PD cooperates with low-concentration rhBMP4 in enhancing retinal differentiation. Moreover, complex NR-RPE organoids with encapsulated NR tissue within RPE were generated by combined treatment with 1.5 nM BMP4 and Chk1i. This PD treatment increased the level of phosphorylated Smad1/5/9 in the inner cells of the aggregate, suggesting that BMP signaling was activated both the outer neuroepithelium and the inner cells. We also confirmed that with long-term *in vitro* culture, PD treated 3D-retina allows generation of retinal cells including rod and cone photoreceptor precursors. These results suggest that the combined use of rhBMP4 and a Chk1i as a retinal differentiation method will be useful for future up-scaling production.

Author contributions

SY conceived the concept of Chk1i treatment and performed experiments and analyzed the data. AKu, AKi, TK originally developed BMP method from feeder-free hPSCs, supervised the retinal differentiation culture, and analyzed the data.

TM and MM and supervised the project and analyzed the data. SY, AKu and MM wrote the manuscript. All authors reviewed the manuscript.

Declaration of competing interest

SY, AKu, AKi and TK are employed by Sumitomo Dainippon Pharma Co., Ltd. M T is a founder and the president of Vision Care Inc.

The authors are co-inventors on patent applications.

Acknowledgements

We thank M. Eiraku and D. Nukaya for the long-term maturation culture of 3D-retina. We thank M. Horiuchi, S. Zeida and T. Senba for conducting *in vitro* experiments. We thank A. Onishi, T. Matsuyama, H-Y. Tu, H, Uyama, Y. Wu, T. Masuda, K. Watari, Y. Kita, and A. Kiso for technical support and members of the M.T. laboratory and

RACMO for discussions. S.Y, A.Ku, A.Ki and T.K are employees of Sumitomo Dainippon Pharma., Ltd; this study was supported by Sumitomo Dainippon Pharma., Ltd. This study was supported by a grant from Japan Agency for Medical Research and Development (AMED) under grant number JP21bm0204002.

Appendix A. Supplementary data

Supplementary data to this article can be found online at https://doi.org/10.1016/j.reth.2021.12.003.

References

[1] Notter MFD, Del Cerro C, Wiegand SJ, Grover DA, Lazar E, Del Cerro M. Intraretinal transplantation for rod-cell replacement in light-damaged retinas. J Neural Transplant 1989;1:1–10. https://doi.org/10.1155/NP.1989.1.
[2] Gouras P, Du J, Gelanze M, Lopez R, Kwun R, Kjeldbye H, et al. Survival and synapse formation of transplanted rat rods. J Neural Transplant Plast 1991;2:91–100. https://doi.org/10.1155/NP.1991.91.
[3] Silverman MS, Hughes SE, Valentino TL, Liu Y. Photoreceptor transplantation: anatomic, electrophysiologic, and behavioral evidence for the functional reconstruction of retinas lacking photoreceptors. Exp Neurol 1992;115:87–94. https://doi.org/10.1016/0014-4886(92)90227-H.
[4] Das T, Del Cerro M, Jalali S, Rao VS, Gullapalli VK, Little C, et al. The transplantation of human fetal neuroretinal cells in advanced retinitis pigmentosa patients: results of a long-term safety study. Exp Neurol 1999;157:58–68. https://doi.org/10.1006/exnr.1998.6992.
[5] Humayun MS, De Juan EJ, Del Cerro M, Dagnelie G, Radner W, Sadda SR, et al. Human neural retinal transplantation. Invest Ophthalmol Vis Sci 2000;41:3100–6.
[6] Radtke ND, Aramant RB, Petry HM, Green PT, Pidwell DJ, Seiler MJ. Vision improvement in retinal degeneration patients by implantation of retina together with retinal pigment epithelium. Am J Ophthalmol 2008;146:172–82. https://doi.org/10.1016/j.ajo.2008.04.009.
[7] Eiraku M, Takata N, Ishibashi H, Kawada M, Sakakura E, Okuda S, et al. Self-organizing optic-cup morphogenesis in three-dimensional culture. Nature 2011;472:51–8. https://doi.org/10.1038/nature09941.
[8] Nakano T, Ando S, Takata N, Kawada M, Muguruma K, Sekiguchi K, et al. Self-formation of optic cups and storable stratified neural retina from human ESCs. Cell Stem Cell 2012;10:771–85. https://doi.org/10.1016/j.stem.2012.05.009.
[9] Kuwahara A, Ozone C, Nakano T, Saito K, Eiraku M, Sasai Y. Generation of a ciliary margin-like stem cell niche from self-organizing human retinal tissue. Nat Commun 2015;6:1–15. https://doi.org/10.1038/ncomms7286.
[10] Fligor CM, Huang KC, Lavekar SS, VanderWall KB, Meyer JS. Differentiation of retinal organoids from human pluripotent stem cells. 1st ed., vol. 159. Elsevier Inc.; 2020. https://doi.org/10.1016/bs.mcb.2020.02.005.
[11] Capowski EE, Samimi K, Mayerl SJ, Phillips MJ, Pinilla I, Howden SE, et al. Reproducibility and staging of 3D human retinal organoids across multiple pluripotent stem cell lines. Development 2019;146:171686. https://doi.org/10.1242/dev.171686.
[12] Chichagova V, Hilgen G, Ghareeb A, Georgiou M, Carter M, Sernagor E, et al. Human iPSC differentiation to retinal organoids in response to IGF1 and BMP4 activation is line- and method-dependent. Stem Cell 2020;38:195–201. https://doi.org/10.1002/stem.3116.
[13] Kuwahara A, Yamasaki S, Mandai M, Watari K, Matsushita K, Fujiwara M, et al. Preconditioning the initial state of feeder-free human pluripotent stem cells promotes self-formation of three-dimensional retinal tissue. Sci Rep 2019;9:1–16. https://doi.org/10.1038/s41598-019-55130-w.
[14] Lin B, McLelland BT, Mathur A, Aramant RB, Seiler MJ. Sheets of human retinal progenitor transplants improve vision in rats with severe retinal degeneration. Exp Eye Res 2018;174:13–28. https://doi.org/10.1016/j.exer.2018.05.017.
[15] McLelland BT, Lin B, Mathur A, Aramant RB, Thomas BB, Nistor G, et al. Transplanted hESC-derived retina organoid sheets differentiate, integrate, and improve visual function in retinal degenerate rats. Invest Ophthalmol Vis Sci 2018;59:2586–603. https://doi.org/10.1167/iovs.17-23646.
[16] Mandai M, Fujii M, Hashiguchi T, Sunagawa GA, Ito S, Sun J, et al. iPSC-derived retina transplants improve vision in rd1 end-stage retinal-degeneration mice. Stem Cell Rep 2017;8:69–83. https://doi.org/10.1016/j.stemcr.2016.12.008.
[17] Shirai H, Mandai M, Matsushita K, Kuwahara A, Yonemura S, Nakano T, et al. Transplantation of human embryonic stem cell-derived retinal tissue in two primate models of retinal degeneration. Proc Natl Acad Sci U S A 2015;113:E81–90. https://doi.org/10.1073/pnas.1512590113.
[18] Iraha S, Tu HY, Yamasaki S, Kagawa T, Goto M, Takahashi R, et al. Establishment of immunodeficient retinal degeneration model mice and functional maturation of human ESC-derived retinal sheets after transplantation. Stem Cell Rep 2018;10:1059–74. https://doi.org/10.1016/j.stemcr.2018.01.032.
[19] Tu HY, Watanabe T, Shirai H, Yamasaki S, Kinoshita M, Matsushita K, et al. Medium- to long-term survival and functional examination of human iPSC-derived retinas in rat and primate models of retinal degeneration. EBioMedicine 2019;39:562–74. https://doi.org/10.1016/j.ebiom.2018.11.028.
[20] Yamasaki S, Sugita S, Horiuchi M, Masuda T, Fujii S, Makabe K, et al. Low immunogenicity and immunosuppressive properties of human ESC- and iPSC-derived retinas. Stem Cell Rep 2021;16:851–67. https://doi.org/10.1016/j.stemcr.2021.02.021.
[21] Walworth N, Davey S, Beach D. Fission yeast chkl protein kinase links the rad checkpoint pathway to cdc2. Nature 1993;363:368–71. https://doi.org/10.1038/363368a0.
[22] Dent P. Investigational CHK1 inhibitors in early phase clinical trials for the treatment of cancer. Expet Opin Invest Drugs 2019;28:1095–100. https://doi.org/10.1080/13543784.2019.1694661.
[23] Feng L, Cook B, Tsai SY, Zhou T, LaFlamme B, Evans T, et al. Discovery of a small-molecule BMP sensitizer for human embryonic stem cell differentiation. Cell Rep 2016;15:2063–75. https://doi.org/10.1016/j.celrep.2016.04.066.
[24] Nakagawa M, Taniguchi Y, Senda S, Takizawa N, Ichisaka T, Asano K, et al. A novel efficient feeder-Free culture system for the derivation of human induced pluripotent stem cells. Sci Rep 2014;4:1–7. https://doi.org/10.1038/srep03594.
[25] Bradford STJ, Ranghini EJ, Grimley E, Lee PH, Dressler GR. High-throughput screens for agonists of bone morphogenetic protein (BMP) signaling identify potent benzoxazole compounds. J Biol Chem 2019;294:3125–36. https://doi.org/10.1074/jbc.RA118.006817.
[26] Genthe JR, Min J, Farmer DM, Shelat AA, Grenet JA, Lin W, et al. Ventromorphins: a new class of small molecule activators of the canonical BMP signaling pathway. ACS Chem Biol 2017;12:2436–47. https://doi.org/10.1021/acschembio.7b00527.
[27] Furukawa T, Kozak CA, Cepko CL. Rax, a novel paired-type homeobox gene, shows expression in the anterior neural fold and developing retina. Proc Natl Acad Sci U S A 1997;94:3088–93. https://doi.org/10.1073/pnas.94.7.3088.
[28] Koshiba-Takeuchi K, Takeuchi JK, Matsumoto K, Momose T, Uno K, Hoepker V, et al. Tbx5 and the retinotectum projection. Science 2000;287:134–7. https://doi.org/10.1126/science.287.5450.134.
[29] Hasegawa Y, Takata N, Okuda S, Kawada M, Eiraku M, Sasai Y. Emergence of dorsal-ventral polarity in ESC-derived retinal tissue. Development 2016;143:3895–906. https://doi.org/10.1242/dev.134601.
[30] Xu RH, Chen X, Li DS, Li R, Addicks GC, Glennon C, et al. BMP4 initiates human embryonic stem cell differentiation to trophoblast. Nat Biotechnol 2002;20:1261–4. https://doi.org/10.1038/nbt761.
[31] Zhang P, Li J, Tan Z, Wang C, Liu T, Chen L, et al. Short-term BMP-4 treatment initiates mesoderm induction in human embryonic stem cells. Blood 2008;111:1933–41. https://doi.org/10.1182/blood-2007-02-074120.
[32] Xu R, Sampsell-barron TL, Gu F, Root S, Peck RM, Pan G, et al. NANOG is a direct target of TGF b/activin-mediated SMAD signaling in human ESCs. Cell Stem Cell 2008;3:196–206. https://doi.org/10.1016/j.stem.2008.07.001.